

Analysis of chiral and thermal susceptibilities

D. Blaschke,¹ A. Höll,¹ C. D. Roberts,² and S. Schmidt¹

¹Fachbereich Physik, Universität Rostock, D-18051 Rostock, Germany

²Physics Division, Building 203, Argonne National Laboratory, Argonne, Illinois 60439-4843

(Received 10 March 1998)

We calculate the chiral and thermal susceptibilities for two confining Dyson-Schwinger equation models of QCD with two light flavors, a quantitative analysis of which yields the critical exponents β and δ that characterize the second-order chiral symmetry restoration transition. The method itself is of interest, minimizing the influence of numerical noise in the calculation of the order parameter for chiral symmetry breaking near the critical temperature. For the more realistic of the two models we estimate $T_c \approx 153$ MeV and the non-mean-field values $\beta = 0.46 \pm 0.04$, $\delta = 4.3 \pm 0.3$, and $1/(\beta\delta) = 0.54 \pm 0.05$, which we discuss in comparison with the results of other models. [S0556-2813(98)04409-4]

PACS number(s): 11.10.Wx, 12.38.Mh, 24.85.+p, 05.70.Fh

I. INTRODUCTION

Phase transitions are characterized by the behavior of an order parameter $\langle X \rangle$, the expectation value of an operator. In the ordered phase of a system, $\langle X \rangle \neq 0$, whereas in the disordered phase $\langle X \rangle = 0$. A phase transition is first order if $\langle X \rangle \rightarrow 0$ discontinuously, whereas it is second order if $\langle X \rangle \rightarrow 0$ continuously. For a second-order transition, the length scale associated with correlations in the system diverges as $\langle X \rangle \rightarrow 0$ and one can define a range of critical exponents that characterize the behavior of certain macroscopic properties at the transition point. For example, in a system that is ferromagnetic for temperatures less than some critical value T_c the magnetization M in the absence of an external magnetic field behaves as $M \propto (T_c - T)^\beta$ for $T \sim T_c^-$, where β is the critical exponent. At the critical temperature the behavior of the magnetization in the presence of an external field $h \rightarrow 0^+$ defines another critical exponent δ : $M \propto h^{1/\delta}$. In a system that can be described by mean field theory these critical exponents are

$$\beta^{\text{MF}} = 0.5, \quad \delta^{\text{MF}} = 3.0. \quad (1)$$

Equilibrium second-order phase transitions can be analyzed using the renormalization group, which leads to scaling laws that reduce the number of independent critical exponents to just 2: β and δ [1]. It is widely conjectured that the values of these exponents are fully determined by the dimension of space and the nature of the order parameter. This is the notion of *universality*, i.e., that the critical exponents are *independent* of a theory's microscopic details and hence all theories can be grouped into a much smaller number of universality classes according to the values of their critical exponents. If this is the case, the behavior of a complicated theory near criticality is completely determined by the behavior of a simpler theory in the same universality class. So, when presented with an apparently complicated theory, the problem is reduced to only that of establishing its universality class.

Quantum chromodynamics is an asymptotically free theory, i.e., there is an intrinsic, renormalization-induced mass scale Λ_{QCD} , and for squared momentum transfer $Q^2 \gg \Lambda_{\text{QCD}}^2$, the interactions between quarks and gluons are

weaker than Coulombic: $\alpha_s(Q^2) \rightarrow 0$ as $Q^2 \rightarrow \infty$. The study of QCD at finite temperature and baryon number density proceeds via the introduction of the intensive variables temperature T and quark chemical potential μ . These are additional mass scales, with which the coupling can *run* and hence, for $T \gg \Lambda_{\text{QCD}}$ and/or $\mu \gg \Lambda_{\text{QCD}}$, $\alpha_s(Q^2 = 0, T, \mu) \sim 0$. It follows that, at finite temperature and/or baryon number density, there is a phase of QCD in which quarks and gluons are weakly interacting, *irrespective* of the momentum transfer [2], i.e., a quark-gluon plasma phase. Such a phase of matter existed approximately one microsecond after the big bang.

At $T, \mu = 0$ the strong interaction is characterized by confinement and dynamical chiral symmetry breaking (DCSB), effects which are tied to the behavior of $\alpha_s(Q^2)$ at small Q^2 , i.e., its long-range behavior. In a phase of QCD in which the coupling is uniformly small for all Q^2 , these effects are absent and the nature of the strong interaction spectrum is qualitatively different.

The path followed in the transition to the plasma is also important because it determines some observational consequences of the plasma's existence. For example [3], the time scale for the expansion of the early universe $\sim 10^{-5}$ s is large compared with the natural time scale in QCD $1/\Lambda_{\text{QCD}} \sim 1 \text{ fm}/c \sim 10^{-23}$ s, hence thermal equilibrium is maintained throughout the QCD transition. Therefore if the transition is second-order the ratio $B := \text{baryon-number/entropy}$ remains unchanged from that value attained at an earlier stage in the universe's evolution. However, a first-order transition would be accompanied by a large increase in entropy density and therefore a reduction in B after the transition. Hence the order of the QCD transition constrains the mechanism for baryon number generation in models describing the formation of the universe, since with a second-order transition this mechanism is only required to produce the presently observed value of B and need not allow for dilution. In the absence of quarks, QCD has a first-order deconfinement transition, while with three or four massless quarks a first-order chiral symmetry restoration transition is expected [3]. What of the realistic case with two light quark flavors?

Based on the global chiral symmetry of QCD with two light quark flavors, it has been argued [3] that this theory and

the $N=4$ Heisenberg magnet are in the same universality class. As a field theory, the $N=4$ Heisenberg magnet is characterized by an interaction of the form

$$\sum_{i=1}^4 \left\{ \frac{1}{2} \mu^2 \phi_i^2(x) + \frac{1}{4} \lambda^4 \phi_i^4(x) \right\}, \quad (2)$$

where μ^2 is a function of temperature: $\mu^2 \geq 0$ at or above the critical temperature T_c^H but $\mu^2 < 0$ for $T < T_c^H$. If the interaction strength λ depends smoothly on T and remains positive, then for $T < T_c^H$ the classical minimum of this potential is at

$$\phi_{\text{cl}}^2 = \frac{-\mu^2}{\lambda} > 0. \quad (3)$$

This model is familiar as the nonlinear σ model, often used to describe low-energy phenomena in QCD. It has been explored thoroughly and has a second-order phase transition with critical exponents [4]

$$\beta^H = 0.38 \pm 0.01, \quad \delta^H = 4.82 \pm 0.05. \quad (4)$$

One can examine the hypothesis that this model and QCD with two light quark flavors are in the same universality class via numerical simulations. Such studies on an $8^3 \times 4$ lattice suggest a second-order chiral phase transition with critical exponents [5]

$$\beta^{\text{lat}} = 0.30 \pm 0.08, \quad \delta^{\text{lat}} = 4.3 \pm 0.5 \quad (5)$$

but do not decide the question.¹ These results were obtained through an analysis of the chiral and thermal susceptibilities, a technique that can be applied in the study of any theory. Herein we illustrate the method via an analysis of two Dyson-Schwinger equation (DSE) models of QCD, which also allows us to explore the hypothesis further.

Dyson-Schwinger equations provide a renormalizable, nonperturbative, continuum framework for the exploration of strong interaction effects. They have been used extensively [7] at $T=0$ in the study of confinement and DCSB, and in the calculation of a wide range of hadron observables [8], including the electroproduction of vector mesons [9] and the semileptonic transition form factors of heavy mesons [10]. They have recently [11,12] found successful application at $T \neq 0$ and it is these two models that we employ as exemplars herein. In Sec. II we describe the models and in Sec. III the analysis of their chiral and thermal susceptibilities, and the evaluation of the associated critical exponents. We summarize and conclude in Sec. IV.

¹A review [6] of results from recent simulations on larger lattices with lighter quarks reports a significant dependence of these critical exponents on the lattice volume but with their product approximately constant. A value of $z_\mu \approx 1 \Rightarrow \delta \rightarrow \infty$ is obtained, which is characteristic of a first-order transition. It suggests that more studies at weaker coupling or with improved actions are necessary in order to understand these unexpected results.

II. TWO MODELS

In order to introduce the DSE models, here we briefly review necessary elements of the DSE formalism: Ref. [7] provides an extensive review and Ref. [13] a heuristic application. We employ a Euclidean metric throughout, with $\{\gamma_\mu, \gamma_\nu\} = 2\delta_{\mu\nu}$ and $\gamma_\mu^\dagger = \gamma_\mu$, in which case the renormalized dressed-quark propagator at $T \neq 0$ takes the form

$$S(p_{\omega_k}) := -i \vec{\gamma} \cdot \vec{p} \vec{\sigma}_A(p_{\omega_k}) - i \gamma_4 \omega_k \sigma_C(p_{\omega_k}) + \sigma_B(p_{\omega_k}), \quad (6)$$

where $(p_{\omega_k}) := (\vec{p}, \omega_k)$ with $\omega_k = (2k+1)\pi T$ the fermion Matsubara frequency, and $\sigma_{\mathcal{F}}(p_{\omega_k})$, $\mathcal{F} = A, B, C$ are functions only of $|\vec{p}|^2$ and ω_k^2 . The propagator is obtained as a solution of the quark DSE

$$S^{-1}(p_{\omega_k}) := i \vec{\gamma} \cdot \vec{p} \vec{A}(p_{\omega_k}) + i \gamma_4 \omega_k C(p_{\omega_k}) + B(p_{\omega_k}) \quad (7)$$

$$= Z_2^A i \vec{\gamma} \cdot \vec{p} + Z_2(i \gamma_4 \omega_k + m_{\text{bm}}) + \Sigma'(p_{\omega_k}), \quad (8)$$

m_{bm} is the Lagrangian current-quark bare mass, and the regularized self-energy is

$$\Sigma'(p_{\omega_k}) = i \vec{\gamma} \cdot \vec{p} \vec{\Sigma}'_A(p_{\omega_k}) + i \gamma_4 \omega_k \Sigma'_C(p_{\omega_k}) + \Sigma'_B(p_{\omega_k}), \quad (9)$$

with

$$\begin{aligned} \Sigma'_{\mathcal{F}}(p_{\omega_k}) &= \int_{l,q}^{\bar{\Lambda}} \frac{4}{3} g^2 D_{\mu\nu}(\vec{p}-\vec{q}, \omega_k - \omega_l) \\ &\quad \times \frac{1}{4} \text{tr}[\mathcal{P}_{\mathcal{F}} \gamma_\mu S(q_{\omega_l}) \Gamma_\nu(q_{\omega_l}; p_{\omega_k})], \end{aligned} \quad (10)$$

where $\mathcal{F} = A, B, C$; $\mathcal{P}_A := -(Z_1^A/|\vec{p}|^2) i \vec{\gamma} \cdot \vec{p}$, $\mathcal{P}_B := Z_1$, $\mathcal{P}_C := -(Z_1/\omega_k) i \gamma_4$; and $\int_{l,q}^{\bar{\Lambda}} := T \sum_{l=-\infty}^{\infty} \int^{\bar{\Lambda}} d^3 q / (2\pi)^3$, with $\int^{\bar{\Lambda}}$ a mnemonic to represent a translationally invariant regularization of the integral and $\bar{\Lambda}$ the regularization mass scale. In Eq. (10), $\Gamma_\nu(q_{\omega_l}; p_{\omega_k})$ is the renormalized dressed-quark-gluon vertex and $D_{\mu\nu}(\vec{p}, \Omega_k)$ is the renormalized dressed-gluon propagator. ($\Omega_k = 2k\pi T$ is the boson Matsubara frequency.)

In renormalizing the quark DSE we require that

$$S^{-1}(p_{\omega_0})|_{|\vec{p}|^2 + \omega_0^2 = \xi^2} = i \vec{\gamma} \cdot \vec{p} + i \gamma_4 \omega_0 + m_R, \quad (11)$$

which entails that the renormalization constants are

$$Z_2^A(\xi, \bar{\Lambda}) = 1 - \Sigma'_A(\xi_{\omega_0}^-; \bar{\Lambda}), \quad (12)$$

$$Z_2(\xi, \bar{\Lambda}) = 1 - \Sigma'_C(\xi_{\omega_0}^-; \bar{\Lambda}), \quad (13)$$

$$m_R(\xi) = Z_2 m_{\text{bm}}(\bar{\Lambda}^2) + \Sigma'_B(\xi_{\omega_0}^-; \bar{\Lambda}), \quad (14)$$

where $(\xi_{\omega_0}^-)^2 := \xi^2 - \omega_0^2$, and the renormalized self-energies are

$$\mathcal{F}(p_{\omega_k}; \xi) = \xi_{\mathcal{F}} + \Sigma'_{\mathcal{F}}(p_{\omega_k}; \bar{\Lambda}) - \Sigma'_{\mathcal{F}}(\xi_{\omega_0}^-; \bar{\Lambda}), \quad (15)$$

$\mathcal{F} = A, B, C$, $\xi_A = 1 = \xi_C$, and $\xi_B = m_R(\xi)$.

So far no approximations or truncations have been made but to continue we must know the form of $\Gamma_\nu(q_{\omega_i}; p_{\omega_k})$ and $D_{\mu\nu}(\vec{p}, \Omega_k)$ in Eq. (10). These Schwinger functions satisfy DSEs. However, the study of those equations is rudimentary even at $T=0$ and there are no studies for $T \neq 0$. To proceed we use the $T=0$ results as a qualitative guide and employ exploratory *Ansätze* for $\Gamma_\nu(q_{\omega_i}; p_{\omega_k})$ and $D_{\mu\nu}(\vec{p}, \Omega_k)$. This is where model parameters enter.

The structure of the dressed fermion-gauge-boson vertex has been much considered [14]. As a connected, irreducible three-point function it should be free of light-cone singularities in covariant gauges, i.e., it should be regular at $(\vec{p} - \vec{q})^2 + (\omega_k - \omega_l)^2 = 0$. A range of *Ansätze* with this property has been proposed and employed [15] and it has become clear that the judicious use of the rainbow truncation

$$\Gamma_\nu(q_{\omega_i}; p_{\omega_k}) = \gamma_\nu \quad (16)$$

in Landau gauge provides reliable results [13]. This is the *Ansatz* employed in Refs. [11,12] and we use it herein. With this truncation a mutually consistent constraint is $Z_1 = Z_2$ and $Z_1^A = Z_2^A$ [13].

With $\Gamma_\nu(q_{\omega_i}; p_{\omega_k})$ regular, the analytic properties of the kernel in the quark DSE are determined by those of $D_{\mu\nu}(p_{\Omega_k})$, which in Landau gauge has the general form

$$g^2 D_{\mu\nu}(p_{\Omega_k}) = P_{\mu\nu}^L(p_{\Omega_k}) \Delta_F(p_{\Omega_k}) + P_{\mu\nu}^T(p_{\Omega_k}) \Delta_G(p_{\Omega_k}), \quad (17)$$

$$P_{\mu\nu}^T(p_{\Omega_k}) \equiv \begin{cases} 0, & \mu \text{ and/or } \nu = 4, \\ \delta_{ij} - \frac{p_i p_j}{p^2}, & \mu, \nu = i, j = 1, 2, 3, \end{cases} \quad (18)$$

with $P_{\mu\nu}^T(p_{\Omega_k}) + P_{\mu\nu}^L(p_{\Omega_k}) = \delta_{\mu\nu} - p_\mu p_\nu / \sum_{\alpha=1}^4 p_\alpha p_\alpha$; $\mu, \nu = 1, \dots, 4$. A ‘‘Debye mass’’ for the gluon appears as a T -dependent contribution to Δ_F . Considering $D_{\mu\nu}(k)$ at $T=0$, a perturbative analysis at two-loop order provides a quantitatively reliable estimate for $k^2 > 1-2 \text{ GeV}^2$, with higher-order terms providing corrections of only $\sim 10\%$. However, for $k^2 < 1 \text{ GeV}^2$ nonperturbative methods are necessary. Studies of the gluon DSE in axial gauge [16], where ghost contributions are absent, or in Landau gauge [17], when their contributions are small, indicate that $D_{\mu\nu}(k)$ is significantly enhanced in the vicinity of $k^2=0$ relative to a free gauge-boson propagator, and that the enhancement persists to $k^2 \sim 1 \text{ GeV}^2$. Due to the truncations involved these studies are not quantitatively reliable but this behavior has been modeled successfully as a distribution located in the vicinity of $k^2=0$ [13,18].

A. Infrared-dominant model

A particularly simple and illustratively useful model is obtained with

$$\Delta_F(p_{\Omega_k}) = \Delta_G(p_{\Omega_k}) = 2\pi^3 \frac{\eta^2}{T} \delta_{k0} \delta^3(\vec{p}), \quad (19)$$

which is a generalization to $T \neq 0$ of the model introduced in Ref. [19], where $\eta \approx 1.06 \text{ GeV}$ is a mass-scale parameter fixed by fitting π - and ρ -meson masses. As an infrared-dominant model Eq. (19) does not represent well the behavior of $D_{\mu\nu}(p_{\Omega_k})$ away from $p_{\Omega_k}^2 \approx 0$, and hence there are some model-dependent artifacts. However, as exemplified in Ref. [12], these artifacts are easily identified and, because of its simplicity, the model provides a useful means of elucidating many of the qualitative features of more sophisticated *Ansätze*.

Using Eqs. (16) and (19) the quark DSE is ultraviolet finite, the cutoff can be removed, and the renormalization point taken to infinity, so that Eq. (8) becomes the algebraic equations

$$\eta^2 m^2 = B^4 + m B^3 + (4p_{\omega_k}^2 - \eta^2 - m^2) B^2 - m(2\eta^2 + m^2 + 4p_{\omega_k}^2) B, \quad (20)$$

$$A(p_{\omega_k}) = C(p_{\omega_k}) = \frac{2B(p_{\omega_k})}{m + B(p_{\omega_k})}, \quad (21)$$

with $Z_2^A = 1 = Z_2$ and $m = m_R = m_{\text{bm}}$: $m=0$ defines the chiral limit. This DSE model of QCD has coincident second-order deconfinement and chiral symmetry restoration phase transitions at a critical temperature $T_c^{\text{IR}} \approx 0.16 \eta$ [12].

B. Ultraviolet-improved model

An improvement over Eq. (19) is obtained by correcting the large- $p_{\Omega_k}^2$ behavior so as to better represent the interaction at short distances. The one-parameter model

$$\Delta_F(p_{\Omega_k}) = \mathcal{D}(p_{\Omega_k}; m_D), \quad (22)$$

$$\Delta_G(p_{\Omega_k}) = \mathcal{D}(p_{\Omega_k}; 0), \quad (23)$$

$$\mathcal{D}(p_{\Omega_k}; m) := \frac{16}{9} \pi^2 \left[\frac{2\pi}{T} m_t^2 \delta_{0k} \delta^3(\vec{p}) + \frac{1 - e^{[-(|\vec{p}|^2 + \Omega_k^2 + m^2)/(4m_t^2)]}}{|\vec{p}|^2 + \Omega_k^2 + m^2} \right], \quad (24)$$

where $m_D^2 = (8/3)\pi^2 T^2$ is the perturbatively evaluated Debye-mass,² achieves this. This gluon propagator provides a generalization to $T \neq 0$ of the model explored in Ref. [18] where the parameter m_t is a mass scale that marks the boundary between the perturbative and nonperturbative domains.

²The influence of the Debye mass on finite- T observables is qualitatively unimportant, even in the vicinity of the chiral symmetry restoration transition. The ratio of the coefficients in the two terms in Eq. (24) is such that the long-range effects associated with $\delta_{0k} \delta^3(p)$ are completely canceled at short distances, i.e., for $|\vec{x}|^2 m_t^2 \ll 1$.

(The infrared-dominant model is recovered in the limit $m_t \rightarrow \infty$; in this limit the interaction is strong at all momentum scales.) The value $m_t = 0.69 \text{ GeV} = 1/0.29 \text{ fm}$ is fixed in Ref. [18] by requiring a good description of a range of π - and ρ -meson properties. In this case the DSE yields a pair of coupled, nonlinear integral equations that must be solved subject to the renormalization boundary conditions, and $m_R = 0$ defines the chiral limit. This model also has coincident second-order deconfinement and chiral symmetry restoration transitions, with the critical temperature $T_c^{\text{UV}} \approx 0.15 \text{ GeV}$ [11].

III. CHIRAL AND THERMAL SUSCEPTIBILITIES

In the study of dynamical chiral symmetry breaking an order parameter often used is the quark condensate $\langle \bar{q}q \rangle_\zeta$. In QCD in the chiral limit this order parameter is defined via the quark propagator [13]:

$$-\langle \bar{q}q \rangle_\zeta := N_c \lim_{\bar{\Lambda} \rightarrow \infty} Z_4(\zeta, \bar{\Lambda}) \times \int_{l,p} \frac{\bar{\Lambda} B_0(p, \omega_l)}{l \cdot p |\vec{p}|^2 A_0(p, \omega_l)^2 + \omega_l^2 C_0(p, \omega_l)^2 + B_0(p, \omega_l)^2}, \quad (25)$$

for each massless quark flavor, where the subscript 0 denotes that the scalar functions A_0, B_0, C_0 are obtained as solutions of Eq. (8) in the chiral limit, and $Z_4(\zeta, \bar{\Lambda})$ is the mass renormalization constant: $Z_4(\zeta, \bar{\Lambda}) m_R(\zeta) = Z_2(\zeta, \bar{\Lambda}) m_{\text{bm}}(\bar{\Lambda})$. The functions have an implicit ζ dependence. From Eq. (25), and as exemplified in Refs. [11–13], it follows that an equivalent order parameter for the chiral transition is

$$\mathcal{X} := B_0(\vec{p}=0, \omega_0), \quad (26)$$

which was used in Refs. [11,12]. Thus the zeroth Matsubara mode determines the character of the chiral phase transition, a conjecture explored in Ref. [20].

To accurately characterize the chiral symmetry restoration transitions in the two models introduced above, we examine closely the chiral and thermal susceptibilities and their scaling behavior near the critical point. This allows a determination of the critical temperature T_c and exponents β and δ , as we explain in the Appendix. In the notation of the Appendix, the ‘‘magnetization’’ is

$$M(t, h) := B(\vec{p}=0, \omega_0), \quad (27)$$

i.e., the value in the infrared of the scalar piece of the quark self-energy obtained as the m_R - and T -dependent solution of Eq. (8).

A. Critical exponents of the infrared-dominant model

In the chiral limit, Eq. (20) has the Nambu-Goldstone mode solution

$$B(p, \omega_k) = \begin{cases} \sqrt{\eta^2 - 4p_{\omega_k}^2}, & p_{\omega_k}^2 < \frac{\eta^2}{4}, \\ 0, & \text{otherwise,} \end{cases} \quad (28)$$

$$C(p, \omega_k) = \begin{cases} 2, & p_{\omega_k}^2 < \frac{\eta^2}{4}, \\ \frac{1}{2} \left(1 + \sqrt{1 + \frac{2\eta^2}{p_{\omega_k}^2}} \right), & \text{otherwise,} \end{cases} \quad (29)$$

and hence

$$M(t, 0) = 2\pi \left(\frac{\eta}{2\pi} + T \right)^{1/2} \left(\frac{\eta}{2\pi} - T \right)^{1/2}. \quad (30)$$

From Eq. (30) we read that

$$T_c^{\text{IR}} = \frac{\eta}{2\pi} \approx 0.159155 \eta, \quad \beta^{\text{IR}} = \frac{1}{2}. \quad (31)$$

To determine δ we use Eq. (20) at $T = T_c$ to obtain

$$\eta^2 m^2 = M(0, h)^4 + m M(0, h)^3 + m^2 M(0, h)^2 - m(3\eta^2 + m^2)M(0, h) \quad (32)$$

and suppose that, for $m \sim 0$, $M(0, h) = a m^{1/\delta}$. Consistency requires

$$\delta^{\text{IR}} = 3. \quad (33)$$

That the chiral symmetry restoration transition in this model is characterized by mean field critical exponents is not surprising because the interaction described by Eq. (19) is a constant in configuration space. Mean field critical exponents are also obtained in chiral random matrix models of QCD [20,21].

To illustrate the evaluation of the critical temperature and exponents using the chiral and thermal susceptibilities we use Eqs. (20), (A9), and (A10) to obtain

$$\chi_h(T, h) = - \frac{2M(T, h)Tb_- [1 - M(T, h)b_-] - M(T, h)Tb_+}{2M(T, h)b_-b_+ [1 - M(T, h)b_-] - b_-b_+ - M(T, h)b_-}, \quad (34)$$

$$\chi_T(T, h) = \frac{8\pi^2 T M(T, h)^2 b_-^2 - 2M(T, h)b_-b_+h [1 - M(T, h)b_-] - M(T, h)hb_+^2}{2M(T, h)b_-b_+ [1 - M(T, h)b_-] - b_-b_+ - M(T, h)b_-}, \quad (35)$$

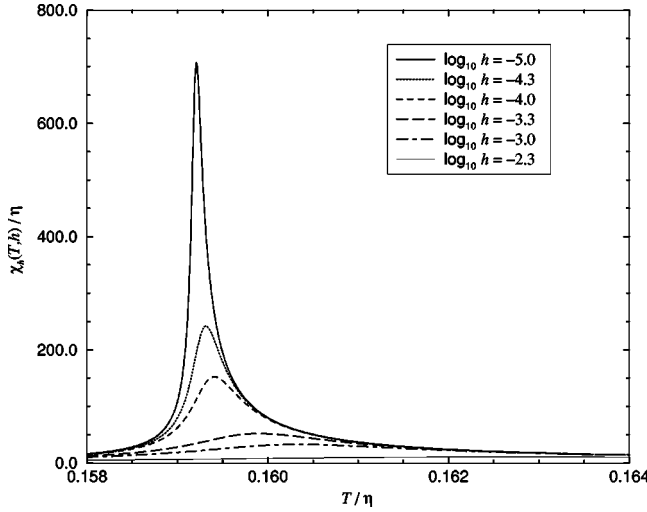


FIG. 1. The chiral susceptibility $\chi_h(T, h)$ in the infrared-dominant model, Eq. (34), as a function of T for various values of h .

where $b_{\pm} := M(T, h) \pm hT$. In Fig. 1 we plot the chiral susceptibility. The temperature dependence is typical of this quantity,³ with the peak increasing in height and becoming narrower as $h \rightarrow 0^+$; i.e., as the external source for chiral symmetry breaking is removed. To understand this behavior, recall that the chiral susceptibility is the derivative of the order parameter with respect to the explicit chiral symmetry breaking mass. Denote the typical mass scale associated with DCSB by M_{χ} . For $m \gg M_{\chi}$, explicit chiral symmetry breaking dominates, with the order parameter $\mathcal{X} \sim m$ and insensitive to T , and hence $\chi_h \approx \text{const}$. For $m \sim M_{\chi}$, \mathcal{X} begins to vary with T because the origin of its magnitude changes from the explicit mass to the DCSB mechanism as T passes through the pseudocritical temperature T_{pc}^h . This is reflected in χ_h as the appearance of a peak at T_{pc}^h . For $m \ll M_{\chi}$, $\mathcal{X} \sim m$ until very near T_{pc}^h when the scale of DCSB overwhelms m and $\mathcal{X} \sim M_{\chi}$. The change in \mathcal{X} is rapid leading to the behavior observed in χ_h . The thermal susceptibility is plotted in Fig. 2 and has qualitatively similar features.

In Table I we present the pseudocritical points and peak heights obtained for h in the scaling window, defined as the domain of h for which

$$\frac{t_{\text{pc}}^h}{t_{\text{pc}}^t} = \text{const}, \quad (36)$$

i.e., the values of h for which Eqs. (A15) and (A16) are valid. Based on Eqs. (A17) and (A18), using the tabulated

³The behavior of the susceptibilities is qualitatively identical to that obtained in lattice simulations, where the massive-quark condensate is used as the chiral order parameter instead of \mathcal{X} in Eq. (26). Small, quantitative differences remain after allowing for the larger quark masses that simulations are limited to. We expect they are due to the different order parameters, e.g., the massive-quark condensate is an integrated quadratically divergent quantity and the associated volume dependence can magnify its intrinsic mass dependence, even after eliminating the simple volume factor. This effect is absent in \mathcal{X} .

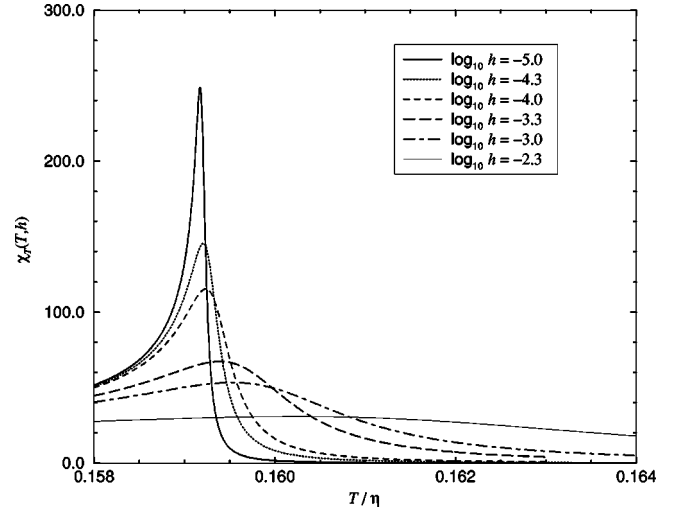


FIG. 2. The thermal susceptibility $\chi_T(T, h)$ in the infrared-dominant model, Eq. (35), as a function of T for various values of h .

values, one obtains z_h^{IR} and z_t^{IR} from linear fits to the curves: $\log_{10} \chi_h^{\text{pc}}$ versus $\log_{10} h$ and $\log_{10} \chi_T^{\text{pc}}$ versus $\log_{10} h$, respectively. This yields

$$z_h^{\text{IR}} = 0.666, \quad z_t^{\text{IR}} = 0.335, \quad (37)$$

and hence $\beta_{\chi}^{\text{IR}} = 0.499$ and $\delta_{\chi}^{\text{IR}} = 2.99$, as listed in Table II. These values are in excellent agreement with the exact (mean field) results, Eqs. (31) and (33). With the value of

$$\frac{1}{(\beta\delta)^{\text{IR}}} = 1 - z_h^{\text{IR}} + z_t^{\text{IR}} = 0.670, \quad (38)$$

T_c^{IR} can be obtained in a variational procedure based on Eq. (A15): it is that value which minimizes the standard deviation between $\log_{10}(T_{\text{pc}}^h - T_c^{\text{IR}}) - 1/(\beta\delta)^{\text{IR}} \log_{10} h$ and a constant. This yields $T_c^{\text{IR}} = 0.159155\eta$ again in excellent agreement with Eq. (31). The value in Table II is obtained with $\eta = 1.06$ GeV [19]. Applying the same procedure to $\log_{10}(T_{\text{pc}}^T - T_c^{\text{IR}}) - 1/(\beta\delta)^{\text{IR}} \log_{10} h$, yields $T_c^{\text{IR}} = 0.159151\eta$.

B. Critical exponents of the ultraviolet-improved model

In this case the quark DSE must be solved numerically, as in Refs. [11,18]. In these calculations we used a three-momentum grid with 96 points and we renormalized at $\zeta = 9.47$ GeV, the value at which the parameter $m_t(\zeta) = 0.69$

TABLE I. The pseudocritical points and peak heights for the chiral and thermal susceptibilities in the infrared-dominant model, obtained from Eqs. (34) and (35), respectively.

$\log_{10} h$	T_{pc}^h/η	χ_h^{pc}/η	T_{pc}^T/η	χ_T^{pc}
-5.0	0.159 21	707.0	0.159 17	248.5
-4.3	0.159 31	241.9	0.159 20	145.4
-4.0	0.159 41	152.9	0.159 23	115.3
-3.3	0.159 90	52.19	0.159 39	67.33
-3.0	0.160 34	32.91	0.159 53	53.34
-2.3	0.162 68	11.31	0.160 52	30.91

TABLE II. Critical exponents and temperature for the models considered herein and a comparison with the results in the $N=4$ Heisenberg magnet [4], labeled as $O(4)$, and the results of lattice simulations of two-light-flavor QCD reported in Ref. [5]. (We list these lattice results only as a guide to a comparison—they are not confirmed by more recent simulations and the correct values of the critical exponents for two-flavor lattice QCD are currently unknown [6].)

	IR dominant	UV improved	$O(4)$	Lattice
δ	3.0	4.3 ± 0.3	4.82 ± 0.05	4.3 ± 0.5
β	0.50	0.46 ± 0.04	0.38 ± 0.01	0.30 ± 0.08
1	0.67	0.54 ± 0.05	0.55 ± 0.02	0.77 ± 0.14
$\beta\delta$				
T_c (MeV)	168.7	153.5 ± 0.1		$140 \dots 160$

GeV) was fixed [18]. The chiral and thermal susceptibilities for a range of values of h are plotted in Figs. 3 and 4, and the pseudocritical points and peak heights obtained for values of h in the scaling window are presented in Table III.

As observed in Sec. III A, one obtains z_h^{UV} and z_t^{UV} from linear fits to the curves $\log_{10} \chi_h^{pc}$ versus $\log_{10} h$ and $\log_{10} \chi_T^{pc}$ versus $\log_{10} h$, respectively. The data and fits are presented in Fig. 5 and yield

$$z_h^{UV} = 0.77 \pm 0.02, \quad z_t^{UV} = 0.28 \pm 0.04, \quad (39)$$

with the corresponding results for β and δ listed in the first column of Table II.⁴ For this model only, as a check and demonstration of consistency, the values of T_c^{UV} and $1/(\beta\delta)^{UV}$ were calculated using a variational procedure based on Eqs. (A15) and (A16): the values of T_c^{UV} and $1/(\beta\delta)^{UV}$ were varied in order to minimize the standard deviation in a linear fit to $\log_{10}(T_{pc} - T_c^{UV}) - 1/(\beta\delta)^{UV} \log_{10} h$. The difference between using T_{pc}^h and T_{pc}^T is less than the error quoted in the table.

In Ref. [11] the values of β and T_c in the ultraviolet-improved model were calculated directly from the magnetization order parameter, i.e., using Eq. (A6), with the results $\beta = 0.33 \pm 0.3$ and $T_c \approx 152$ MeV. There is a discrepancy in the value of β . We expect that the result obtained herein is more accurate because our method avoids the numerical noise associated with establishing the precise behavior of the order parameter in the vicinity of the critical temperature.

IV. SUMMARY AND CONCLUSIONS

A primary purpose of this study was an illustration of the method by which one can calculate the critical exponents that characterize a chiral symmetry restoration transition, β and δ , using the chiral and thermal susceptibilities. For this purpose we chose two Dyson-Schwinger equation models of two-light-flavor QCD that have been applied successfully

⁴Our quoted error bounds the slope of the linear fit. It is calculated from the slope of linear fits to the two end-point values when they are displaced vertically, in opposite directions, by the standard deviation of the fit to all the tabulated results.

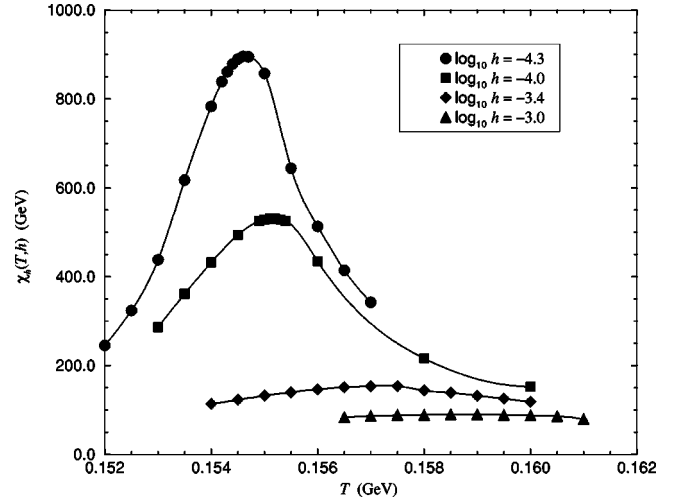


FIG. 3. The chiral susceptibility $\chi_c(T, h)$ in the ultraviolet-improved model, Sec. II B, as a function of T for various values of h .

[11,12,22] in phenomenological studies of QCD at finite temperature and density. The method is reliable and should have a wide range of applications because it is more accurate in the presence of numerical noise than a straightforward analysis of the chiral symmetry (magnetization) order parameter.

We established that our finite temperature extension of the infrared-dominant model of Ref. [19] is characterized by mean field critical exponents, listed in Table II. It is therefore not in the universality class anticipated [3] for two-light-flavor lattice QCD. However, the critical temperature is consistent with that estimated in lattice simulations. This fits an emerging pattern that DSE models whose mass-scale parameters are fixed by requiring a good description of hadron observables at $T=0$, yield a reliable estimate of the critical temperature for chiral symmetry restoration. It is a quantity that is not too sensitive to details of the model.

Consistent with this observation, the critical temperature in the ultraviolet improved model of Ref. [18] also agrees with that estimated in lattice simulations. For the critical ex-

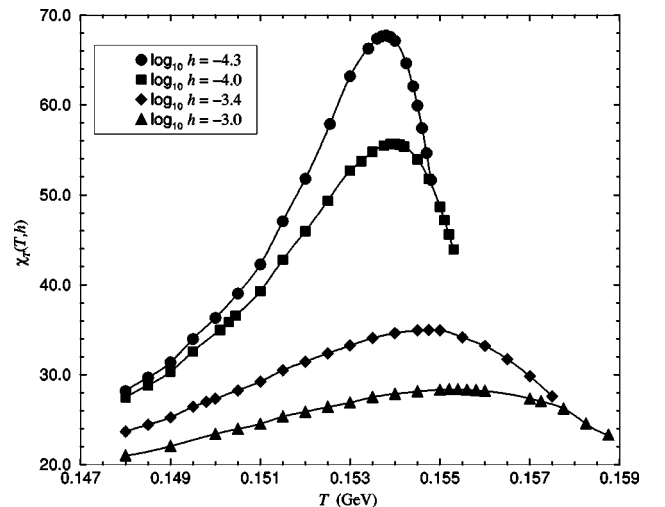


FIG. 4. The thermal susceptibility $\chi_T(T, h)$ in the ultraviolet-improved model, Sec. II B, as a function of T for various values of h .

TABLE III. The pseudocritical points and peak heights for the chiral and thermal susceptibilities in the ultraviolet-improved model, obtained from the numerical solution of Eq. (8) with the gluon propagator of Eqs. (22)–(24). From the dependence of the peak heights on the number of points in the \vec{p} array, we estimate a systematic 1.5% error in χ_h^{pc} and 10% in χ_T^{pc} .

$\log_{10}h$	T_{pc}^h (GeV)	χ_h^{pc} (GeV)	T_{pc}^T (GeV)	χ_T^{pc}
-4.30	0.154 64	896.3	0.153 79	67.72
-4.00	0.155 15	530.7	0.153 94	55.70
-3.70	0.155 71	303.8	0.154 22	45.70
-3.52	0.156 27	224.9	0.154 43	40.65
-3.40	0.156 77	181.8	0.154 60	37.37
-3.30	0.157 29	154.9	0.154 87	35.00
-3.15	0.157 95	120.3	0.155 08	31.64
-3.04	0.158 40	97.21	0.155 34	29.32
-3.0	0.158 72	90.03	0.155 36	28.39

ponents, δ agrees with that obtained in the simulations of two-light-flavor lattice QCD in Ref. [5], but β differs, and this is unlikely to be due to numerical errors in our study. Unfortunately, this discrepancy cannot presently be used either as a guide to improving our DSE model or as a check of the results of lattice simulations because the critical exponents reported in Ref. [5] are not confirmed by recent studies using larger lattices and smaller fermion masses [6]. The correct values of the critical exponents for two-light-flavor lattice QCD are currently unknown. A firm conclusion is that the ultraviolet-improved DSE model is not in the same universality class as the $N=4$ Heisenberg magnet. It therefore illustrates the fact that there are many theories providing a good description of low-energy π and ρ observables which are not in that universality class.

In this and its comparison with the IR-dominant model, it suggests that a determination of the critical exponents of QCD may require a greater understanding of QCD dynamics than has been anticipated. To elucidate, the difference between the infrared-dominant model and the ultraviolet-improved one is the value of m_t , i.e., the mass scale marking the boundary between strong and weak coupling. The ultraviolet-improved model evolves continuously into the infrared-dominant one as $m_t \rightarrow \infty$, in which limit the interaction is always strong. The particular manner in which the theory evolves from weak to strong coupling is characterized by the magnitude of m_t , and our results suggest that the critical exponents are sensitive to the details of this evolution. This is plausible since that evolution is a determining characteristic of the β function of a renormalizable theory, one which could influence a chiral symmetry restoration transition.

The large- p^2 behavior of the gluon propagator in the ultraviolet-improved model, although better than that in the infrared-dominant model, is still inadequate. Its renormalization group properties are more similar to those of quenched QED than QCD because of the absence of the logarithmic suppression of the running coupling characteristic of asymptotically free theories. This is corrected in the model of Ref. [13], which has more in common with QCD at $T=0$ and whose finite temperature properties can therefore assist in better understanding the details of the chiral symmetry res-

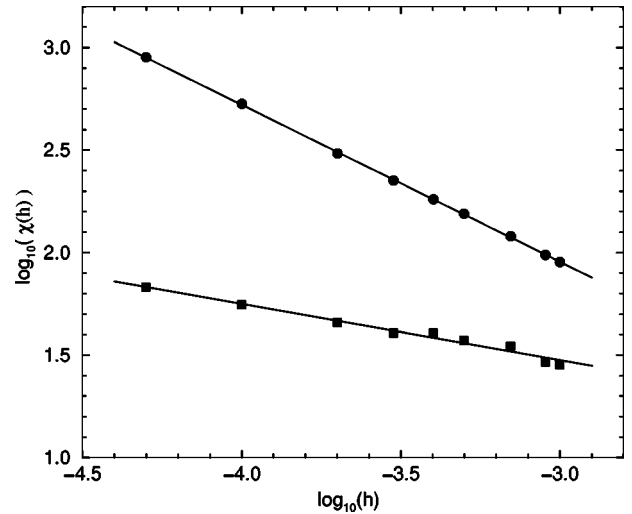


FIG. 5. The peak heights at the pseudocritical points of the chiral and thermal susceptibilities in the ultraviolet-improved model: χ_h^{pc} (filled circles), χ_T^{pc} (filled squares). The solid lines are straight-line fits, with the slopes $-z_h^{\text{UV}}$ and $-z_t^{\text{UV}}$ given in Eq. (39), which verify the scaling laws in Eqs. (A17) and (A18).

toration transition in two-light-flavor QCD. Hence it is better suited to cross checking and improvement by comparison with lattice simulations, and the extrapolation of the results of lattice-QCD studies into that domain which is presently inaccessible, such as finite chemical potential and the T and μ dependence of hadron properties. These applications are currently being pursued.

ACKNOWLEDGMENTS

D.B. and S.S. acknowledge the hospitality of the Physics Division at Argonne National Laboratory, and C.D.R. that of the Department of Physics at the University of Rostock during visits in which parts of this work were conducted. We are also grateful to the faculty and staff at JINR-Dubna for their hospitality during the workshop on *Deconfinement at Finite Temperature and Density* in October 1997. This work was supported in part by Deutscher Akademischer Austauschdienst, the U.S. Department of Energy, Nuclear Physics Division, under Contract No. W-31-109-ENG-38, the National Science Foundation under Grant No. INT-9603385, and benefited from the resources of the National Energy Research Scientific Computing Center.

APPENDIX: CRITICAL EXPONENTS FROM SUSCEPTIBILITIES

Consider the free energy of a theory, represented by

$$f = f(t, h), \quad (\text{A1})$$

where $t := T/T_c - 1$ is the reduced temperature and $h := m/T$ is the explicit source of chiral symmetry breaking measured in units of the temperature. It is analogous to an external magnetic field. Since correlation lengths diverge in a second-order transition it follows that for $t, h \rightarrow 0$ the free energy is a generalized homogeneous function, i.e.,

$$f(t,h) = \frac{1}{b} f(tb^{y_t}, hb^{y_h}). \quad (\text{A2})$$

This entails the following behavior of the ‘‘magnetization’’

$$M(t,h) := \left. \frac{\partial f(t,h)}{\partial h} \right|_{t \text{ fixed}}, \quad (\text{A3})$$

$$M(t,h) = b^{y_h-1} M(tb^{y_t}, hb^{y_h}). \quad (\text{A4})$$

The scaling parameter b is arbitrary and along the trajectory $|t|b^{y_t} = 1$ one has

$$M(t,h) = |t|^{(1-y_h)/y_t} M(\text{sgn}(t), h|t|^{-y_h/y_t}), \quad (\text{A5})$$

$$M(t,0) \propto |t|^\beta, \quad \beta := \frac{1-y_h}{y_t}. \quad (\text{A6})$$

Alternatively, along the trajectory $hb^{y_h} = 1$,

$$M(t,h) = h^{(1-y_h)/y_h} M(th^{-y_t/y_h}, 1), \quad (\text{A7})$$

$$M(0,h) \propto h^{1/\delta}, \quad \delta := \frac{y_h}{1-y_h}. \quad (\text{A8})$$

This defines the critical behavior and provides that direct means of extracting the critical exponent β employed in Refs. [11,12]. However, because of numerical noise, it can be difficult to extract quantitatively accurate results using this method.

The critical exponents can also be determined by studying the pseudocritical behavior of the chiral and thermal susceptibilities, defined respectively as

$$\chi_h(t,h) := \left. \frac{\partial M(t,h)}{\partial h} \right|_{t \text{ fixed}}, \quad (\text{A9})$$

$$\chi_t(t,h) := \left. \frac{\partial M(t,h)}{\partial t} \right|_{h \text{ fixed}}. \quad (\text{A10})$$

For convenience, we often use $\chi_T(T,h) := (1/T_c)\chi_t(t,h)$.

For $t, h \rightarrow 0^+$, along $hb^{y_h} = 1$, one has

$$\chi_h(t,h) = h^{(1-2y_h)/y_h} \chi_h(th^{-y_t/y_h}, 1), \quad (\text{A11})$$

$$\chi_t(t,h) = h^{(1-y_h-y_t)/y_h} \chi_t(th^{-y_t/y_h}, 1). \quad (\text{A12})$$

At each h , $\chi_h(t,h)$ and $\chi_t(t,h)$ are smooth functions of t . Suppose they have maxima at t_{pc}^h and t_{pc}^t , respectively, described as the pseudocritical points. Consider the chiral susceptibility. At its maximum

$$0 = \left. \frac{\partial}{\partial t} \chi_h(t,h) \right|_{t_{pc}^h} \quad (\text{A13})$$

$$= h^{(1-2y_h)/y_h} \left. \frac{\partial}{\partial t} (th^{-y_t/y_h}) \left[\frac{\partial}{\partial z} \chi_h(z,1) \right] \right|_{z=th^{-y_t/y_h}} \bigg|_{t_{pc}^h}, \quad (\text{A14})$$

which entails that

$$t_{pc}^h = K_h h^{y_t/y_h} = K_h h^{1/(\beta\delta)}, \quad (\text{A15})$$

where K_h is an undetermined constant. Similarly,

$$t_{pc}^t = K_t h^{y_t/y_h} = K_t h^{1/(\beta\delta)}. \quad (\text{A16})$$

Since $\beta\delta > 0$, it follows that the pseudocritical points approach the critical point, $t=0$, as $h \rightarrow 0^+$. It follows from Eqs. (A15) and (A16) that at the pseudocritical points

$$\chi_h^{pc} := \chi_h(t_{pc}^h, h) \propto h^{-z_h}, \quad z_h := 1 - \frac{1}{\delta}, \quad (\text{A17})$$

$$\chi_t^{pc} := \chi_t(t_{pc}^t, h) \propto h^{-z_t}, \quad z_t := \frac{1}{\beta\delta} (1 - \beta). \quad (\text{A18})$$

Thus by locating the pseudocritical points and plotting the peak height of the susceptibilities as a function of h one can obtain values of T_c , β , and δ .

[1] R. J. Creswick, H. A. Farach, and C. P. Poole, *Introduction to Renormalization Group Methods in Physics* (Wiley, New York, 1992).
 [2] J. C. Collins and M. J. Perry, Phys. Rev. Lett. **34**, 1353 (1975).
 [3] K. Rajagopal, in *Quark-gluon Plasma*, edited by R. C. Hwa (World Scientific, New York, 1995), p. 484.
 [4] G. Baker, B. Nickel, and D. Meiron, Phys. Rev. B **17**, 1365 (1978); University of Guelph report, 1977 (unpublished).
 [5] F. Karsch and E. Laermann, Phys. Rev. D **50**, 6954 (1994).
 [6] E. Laermann, hep-lat/9802030.
 [7] C. D. Roberts and A. G. Williams, Prog. Part. Nucl. Phys. **33**, 477 (1994).
 [8] P. C. Tandy, Prog. Part. Nucl. Phys. **39**, 117 (1997).
 [9] M. A. Pichowsky and T.-S. H. Lee, Phys. Rev. D **56**, 1644 (1997).
 [10] M. A. Ivanov, Yu. L. Kalinovsky, P. Maris, and C. D. Roberts, Phys. Rev. C **57**, 1991 (1998).

[11] A. Bender, D. Blaschke, Yu. Kalinovsky, and C. D. Roberts, Phys. Rev. Lett. **77**, 3724 (1996).
 [12] D. Blaschke, C. D. Roberts, and S. Schmidt, Phys. Lett. B **425**, 232 (1998).
 [13] P. Maris and C. D. Roberts, Phys. Rev. C **56**, 3369 (1997).
 [14] A. Bashir, A. Kizilersu, and M. R. Pennington, Phys. Rev. D **57**, 1242 (1998).
 [15] F. T. Hawes, C. D. Roberts, and A. G. Williams, Phys. Rev. D **49**, 4683 (1994).
 [16] M. Baker, J. S. Ball, and F. Zachariasen, Nucl. Phys. **B186**, 531 (1981); **B186**, 560 (1981); D. Atkinson, P. W. Johnson, W. J. Schoenmaker, and H. A. Slim, Nuovo Cimento A **77**, 197 (1983).
 [17] N. Brown and M. R. Pennington, Phys. Rev. D **39**, 2723 (1989); M. R. Pennington, hep-ph/9611242.
 [18] M. R. Frank and C. D. Roberts, Phys. Rev. C **53**, 390 (1996).
 [19] H. J. Munczek and A. M. Nemirovsky, Phys. Rev. D **28**, 181 (1983).

- [20] A. D. Jackson and J. J. M. Verbaarschot, *Phys. Rev. D* **53**, 7223 (1996).
- [21] T. Wettig, T. Guhr, A. Schäfer, and H. A. Weidenmüller, in “QCD Phase Transitions,” Proceedings of the XXVth International Workshop on Gross Properties of Nuclei and Nuclear Excitations, Hirschegg, Austria, 1997, edited by H. Feldmeier, J. Knoll, W. Nörenberg, and J. Wambach, hep-ph/9701387.
- [22] A. Bender, G. Poulis, C. D. Roberts, S. Schmidt, and A. W. Thomas, *Phys Lett. B* **431**, 263 (1998).